Fuel 367 (2024) 131501

Contents lists available at ScienceDirect

Fuel

journal homepage: www.elsevier.com/locate/fuel

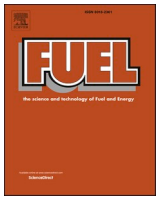

Full Length Article

Assessing the influence of biomass origin and fractionation methods on pyrolysis of primary biomass fractions

N. Almagro-Herrera, S. Lozano-Calvo *, A. Palma, J.C. García, M.J. Díaz

Research Centre for Technology of Products and Chemical Processes (PRO^{2}TECS), Department of Chemical Engineering, University of Huelva, Av. 3 de marzo s/n, 21071 Huelva, Spain

ARTICLE INFO

Keywords:
Activation energy
Fractionation methods
Lignocellulosic biomass
Pyrolysis gases
TD/GC–MS

ABSTRACT

Pyrolysis has emerged as a highly promising technology for the efficient utilization of organic materials, particularly lignocellulosic materials. This study investigates the behavior and influence of three primary biomass fractions (cellulose, hemicellulose, and lignin) derived from different sources (trees, shrubs, and agricultural residues) on the kinetic of the pyrolysis process. With this objective, different fragmentation methods were employed to isolate the main components of the lignocellulosic biomass, followed by thermogravimetric analysis to examine the pyrolysis process. The activation energy was determined using both, the Friedman differential kinetic models of and the Flynn-Wall-Ozawa integrated method, with the latter being found to be more efficient. The activation energy (Ea) was found to be influenced by several factors, including the fractionation process and the origin of the raw material. For hemicellulose, the Ea was in the range of 200–300 kJ mol^{-1}, while cellulose showed Ea values of about 180–220 kJ mol^{-1}. In contrast, lignin displayed a wider range of Ea variation, with its values being more sensitive to the fractionation method used. Gas samples were collected through adsorption tubes during pyrolysis for analysis of gas stream compositions from different lignocellulosic fractions using gas chromatography/mass spectrometry. Furfural, among other compounds, was predominantly detected in the pyrolysis of hemicellulose fractions, ranging from 6.6 % to 19.3 %.

1. Introduction

Biomass can be used as an alternative to fossil fuels to reduce greenhouse gas emissions and promote sustainable development [1]. One of the most promising uses is to produce fuels such as bio-oil, renewable diesel, methane, and hydrogen through processes such as pyrolysis and hydrotreatment [2].Biomass can also be used to produce a range of valuable chemicals, materials and products through biorefineries, similar to oil refineries and petrochemical plants [3]. These processes have both positive and negative ecological impacts, and therefore need to be optimized from both a technical and economic point of view [4,5].

In this context, in order to successfully achieve biomass valorisation, there are several needs that must be addressed, among which stand out (i) the optimisation of pre-treatments due to the fact that biomass is a complex and recalcitrant material that must undergo pre-treatment to decompose its structure and make it more accessible to conversion processes [6]; (ii)the selection of the optimal valorisation technology depending on the characteristics of the biomass [7,8]; and (iii) the proper integration of the technology used with existing industries such as agriculture, forestry and biorefineries. This approach can also contribute to the creation of a circular economy in which waste materials are transformed into valuable products [9].

There are numerous technologies for biomass valorisation, such as direct combustion, biochemicals such as fermentation or anaerobic digestion, and thermochemical including pyrolysis, gasification, or hydrothermal liquefaction. Among them, pyrolysis is an efficient thermochemical process that can convert biomass into pyrolytic gas, bio-oil and solid biochar, meeting the requirements mentioned above [10,11]. In general, the pyrolysis process involves heating biomass in the absence of oxygen to temperatures between 300 and 800 °C. In addition, the pyrolysis process can be easily integrated with other biomass valorisation processes, such as anaerobic digestion, to increase the overall biomass conversion efficiency [12].

The kinetics of the pyrolysis process, regulated by reaction rate, temperature, and residence time, must be carefully controlled to optimize the yield and quality of the pyrolysis products. Biomass composition, primarily comprising cellulose, hemicelluloses, and lignin, has a

* Corresponding author.
E-mail address: susana.lozano@diq.uhu.es (S. Lozano-Calvo).

https://doi.org/10.1016/j.fuel.2024.131501
Received 12 December 2023; Received in revised form 13 March 2024; Accepted 15 March 2024
Available online 16 March 2024

significant influence on pyrolysis rate and efficiency [13]. These polymers have different physical behavior and thermochemical properties depending on feedstock, biomass, and other required properties [14]. Furthermore, significant variations in biomass behavior during pyrolysis arise from differences in the structure and chemistry of polymers, resulting in different decomposition ratios, temperatures, and forms [15].The operating variables of the pyrolysis process must be carefully controlled to optimize its efficiency. For example, higher temperatures tend to increase the yield of gaseous products, whereas lower temperatures favor the production of liquid bio-oil [16]. Similarly, longer residence times result in higher char yield, while shorter residence times enhance the yield of gaseous and liquid products [17]. In pyrolysis, the key operating variables are the temperature and the activation energy, which vary depending on the biomass components. Some studies suggest that the activation energy depends on the degree of polymerisation of the components [13].

Consequently, understanding the influence of biomass composition and pyrolysis process kinetics are critical factors. In this sense, the relative influence of each of the fractions on the kinetics of the process, and therefore on the products generated, has not been studied in depth. Some articles with pure compounds have been found [16,18–20], but no comparison of the comparative influence between different types of cellulose, hemicelluloses and lignin has been made.

In order to understand the impact of each major fraction lignocellulosic biomass, it is essential to fragment the biomass. Various treatments can be used sequentially for this purpose. One such treatmentis cold alkaline extraction, which offers operational and environmental advantages as it operates below 40 °C [21]. Other methods that can be utilized include the kraft and soda-anthraquinone processes to obtain the cellulosic and lignocellulosic fraction. The kraft process, a traditional and widely used method, solubilizes more than half of the hemicelluloses and almost all of the lignin from the fibers, while the cellulose undergoes partial degradation without dissolution, leading to an increase in its crystallinity degree [22–24]. Alternatively, soda-anthraquinone, serves as an alkaline, non-sulphur alternative to the kraft process. However, the cellulose pulp produced by the soda-anthraquinone process has lower strength compared to kraft [25].

The aim of this study is, therefore, to explore the comparative valorization of the pyrolysis (kinetic, and gasses) of the main biomass fractions (cellulose, hemicellulose, lignin) with different characteristics and origins (tree, shrub, agricultural residue) and under different types of fractionations (kraft and soda-anthraquinone), focusing on its potential applications.

2. Materials and methods

2.1. Materials

Three types of biomasses with different characteristics and compositions have been evaluated. *Populus x-Euroamericana* clone AF2 (Poplar) as a tree, Tagasaste as a shrub (because both are high-yielding species) and Wheat Straw as agroforestry waste have been selected. The Agroforestry Department of University of Huelva has supplied these raw materials. For all the raw materials studied, the initial conditioning consists of a mechanical treatment based on the reduction of the sliver size that runs on a disposer conventional (Mill Retsch) with a sieve of mesh size 20 mm and, later, sieved to obtain the length and width average of chips between 1 and 3 cm and 0.5 cm, respectively. Finally, the chips are stored at room temperature to maintain a constant moisture level and then packed in airtight containers. The main chemical characteristics of the materials used in Table 1 are shown, and the main parameters of industrial interest and elemental analysis of the biomasses under study in Table 2 are shown.

Table 1
Chemical characterization of studied raw materials.

Characterization/Raw Material	Poplar	Tagasaste	Wheat Straw
Removable in ethanol (% p/p)	12.13 ± 1.32	11.36 ± 1.10	20.35 ± 4.23
Glucan (% p/p)	40.31 ± 5.15	41.42 ± 4.02	34.12 ± 6.86
Xylan (% p/p)	19.35 ± 1.04	18.56 ± 1.25	14.33 ± 4.14
Araban (% p/p)	0.23 ± 0.15	0.65 ± 0.21	2.35 ± 0.15
Acetyl Groups (% p/p)	2.88 ± 0.39	3.31 ± 0.17	2.12 ± 0.17
Lignin Klason (% p/p)	19.53 ± 1.65	20.1 ± 1.72	21.62 ± 2.38
Ash (% p/p)	1.4 ± 1.41	0.8 ± 0.90	4.02 ± 0.31

Table 2
Proximate, ultimate and calorific values for studied biomasses.

	Proximate[a]		Ultimate[b]			Calorimetry[c]
	Volatile (%)	Fixed Carbon (%)	H (%)	C (%)	N (%)	HHV (MJ/kg)
Poplar	85.61 ± 2.3	12.30 ± 0.4	6.21 ± 0.2	48.68 ± 0.7	1.05 ± 0.1	14.35 ± 1.2
Tagasaste	78.84 ± 1.9	18.65 ± 0.8	6.58 ± 0.2	47.31 ± 0.9	4.23 ± 0.1	16.27 ± 1.5
Wheat Straw	73.55 ± 1.2	15.21 ± 0.5	5.41 ± 0.2	43.16 ± 0.6	0.30 ± 0.1	16.82 ± 1.3

[a] Proximate analysis was done according to ASTM D5142-09.
[b] Ultimate analysis was conducted using a modified ASTM D5373-10 method.
[c] Heating value (HHV) were determined with a calorimeter using ASTM D5865-10.

2.2. Biomass treatments

Three replicates for each of the tested treatments have been performed.

2.2.1. Alkali Pretreatment: Hemicellulose extraction

Alkaline pretreatments are used in biorefinery for delignification to improve the accessibility and digestibility of polysaccharides as a step before enzymatic hydrolysis or microbial digestion [26]. Among the alkaline treatments, cold alkaline extraction (CAE) is widely used. This operation breaks down the biomass into hemicelluloses and soluble lignins in alkali and waste through the separation of heteropolysaccharides polymer of the fiber source. In this way, it facilitates the use of these components in higher value products with minimal chemical and physical changes. In this case, the hemicelluloses are extracted from the biomass in the liquor with a polymeric structure without significant degradation [27,28]. The used conditions were: 40 °C operating temperature; 90 min operating time and 100 $g.L^{-1}$ alkali concentration for Wheat Straw [27] and 120 $g.L^{-1}$ for Tagasaste and Poplar [29]. The difference lies in the type of lignocellulosic biomass. Wheat is herbaceous and has a greater capacity for hemicelluloses extraction, while the nature of the others requires a higher alkali concentration to extract the hemicelluloses. The resulting solid from the cold alkaline extraction is repeatedly washed with water to remove any traces of NaOH according to TAPPI standard T264 cm-07 [30].

2.2.2. Delignification kraft treatment

The solid obtained is the cellulose-rich pre-treatment and contains most of the lignin from the biomass. The kraft process is currently the dominant delignification method for paper pulp production due to its advantages over other methods for the same purpose [31]. The operating conditions for a batch pulp mill were as follows: a liquid to solid ratio of 3.5; a sulphide content of 25 %, a cooking temperature of 165 °C and a cooking time of 50 min [32].

2.2.3. Delignification soda-anthraquinone treatment

Among the alternative methods, the most widely used is an alkaline

(NaOH), sulphur-free process using anthraquinone (AQ) as a catalyst. The cellulose obtained is more difficult to bleach and has poorer resistance properties than that obtained by the kraft process [33]. For this delignification process, 13 % active alkali; a temperature of 143 °C and a time of 90 min for all the biomasses studied [32] has been used.

2.2.4. Chemical analysis

The standards: TAPPI T264 cm-07 [30] to determine the moisture content of the raw material; TAPPI T204 cm-07 [33] standard to measure extractable compounds such as hydrocarbons, non-volatile low molecular weight carbohydrates, phytosterols, salts, waxes, polyphenols, resins, fats and other compounds; TAPPI T222 [34] for the quantitative determination of monomeric compounds and lignin and TAPPI T249 [35] to the determination of monomeric sugars, i.e. xylose, glucose and arabinose, acetic acid and possibly 5-hydroxymethylfurfural and furfural by HPLC, have been successfully used.

2.3. Thermogravimetric analysis

The thermogravimetric experiments applied to each of the different biomasses and fractions studied were carried out on the Mettler Toledo TGA/DSC1 STARe system. The samples of the different starting materials were previously ground and homogenized. In the pyrolysis experiments, nitrogen was used as an inert gas to avoid secondary reactions. The pyrolysis processes were carried out in two steps: (i) heating the sample from 25 to 105 °C with a heating rate of 15 °C min^{-1} and an inert nitrogen atmosphere with a flow rate of 15 mL min^{-1}; (ii) heating from 105 to 800 °C with different heating rates (5, 10, 15, 20 and 25 °C min^{-1}) with a nitrogen flow rate of 30 mL min^{-1}. The initial sample mass was approximately 10 mg in all cases and the experiments were carried out in triplicate and the mean values recorded.

2.4. Kinetic models

Iso-conversional kinetic methods are those in which the variation of the activation energy is estimated as a function of the conversion degree. These models are of great importance in systems where there is a variation of the activation energy as a function of the conversion degree. This type of method is particularly useful for biomass, which degrades at different temperatures due to the diverse and heterogeneous nature of its components [36]. Within this type, there are two groups: differential methods and integral methods [37]. These models are used to determine the kinetic parameters of the reaction by using the Arrhenius equation (Eq. (1), and that all the reactions are of order 1, because there is an excess of the sample, in these models are assumed.

$$k(T) = Ae^{\left(\frac{-E_a}{RT}\right)} \tag{1}$$

Where: A: preexponential factor (s^{-1}); E_a: activation energy (kJ mol^{-1})); and R: universal gas constant (8,8145 kJ mol^{-1}K).

In general, in the differential kinetic models data from dα/dt as a function of T (Eq.2) are fitted.

$$\frac{d\alpha}{dt} = Ae^{\left(\frac{-E_a}{RT}\right)} f(\alpha) \tag{2}$$

Where: dα/dt: ratio of reaction, represented as the variation of the conversion (α), calculated through the loss of mass, with respect to time (t); and f(α): dependent on temperature (T) function of the conversion.

However, when working in conditions that are not isothermal, the temperature will vary with time and will produce a specific heating rate (β) and the Eq. (3) will be obtained.

$$\frac{d\alpha}{dT} = \frac{A}{\beta}e^{\left(\frac{-E_a}{RT}\right)} f(\alpha) \tag{3}$$

Integral methods, by separating the variables and integrating with respect to the limits α and 0; T and T0, which is then simplified to 0 since the reaction ratio is significant from the initial temperature, Eq. (4) can be obtained.

$$g(\alpha) = \int_0^\alpha \frac{d\alpha}{dT} = \frac{A}{\beta}\int_{T_0}^{T} e^{\left(\frac{-E_a}{RT}\right)} dT \approx \frac{A}{\beta}\int_0^T e^{\left(\frac{-E_a}{RT}\right)} dT \tag{4}$$

g(α): conversion dependent function.

The integrated models used data α, or an integral of α as a function of t, or T. In this sense, the Flynn-Wall-Ozawa (FWO) method [38,39], which faithfully represents systems where there is more than one simultaneous reaction [40]. The equation for this method is shown in Eq. (5).

$$ln(\beta) = ln\left(\frac{AE_a}{Rg(\alpha)}\right) = 5,523 - 1,052\left(\frac{E_a}{RT}\right) \tag{5}$$

Using the Eq. (5) for each of the conversion degrees, we get the Eq. (6).

$$ln(\beta) = ln\left(\frac{AE_a}{R}\right) - lng(\alpha) - 0,4567\left(\frac{E_a}{RT}\right) \tag{6}$$

For each conversion value (α), by plotting lnβ versus 1/T, a line with a slope of −0.4567 E_a/R can be obtained and the activation energy calculated. The pre-exponential factor (A) can be found by intersecting the line with the axes.

On the other hand, the values of the DTG curve (Differential Thermogravimetric Analysis) are used for the differential methods. The method developed by Friedman [41] is the most widely used differential method. This method is based on the application of logarithms to equation (3), which results in Eq. (7).

$$ln\left(\beta\frac{d\alpha}{dT}\right) = ln\left(\frac{d\alpha}{dt}\right) = ln[Af(\alpha)]\frac{-E_a}{RT} \tag{7}$$

For each conversion degree (a) and heating rate (b), the plot of ln(dα/dt) versus 1/T gives a straight line whose slope is -E_a/R. From this slope, the value of the activation energy for each of the conversions is determined [40].

2.5. Pyrolysis products analysis by TD/GC–MS

To obtain the pyrolysis products (pyrolytic gases) from different fractions (cellulose, hemicellulose, and lignin) of the three biomass species studied, a laboratory-scale reactor was used. The reactor comprises a temperature-controlled furnace housing a quartz tube measuring 10 mm in diameter and 140 cm in length. A horizontal actuator is employed to introduce the sample, typically around 1 g. The residence time was systematically set a 7 min and nitrogen (250 cm^3 min^{-1}) was used as transport gas.

Volatile compounds samples from the pyrolysis process at the peak temperature ranges of the different biomasses and fractions obtained (hemicellulose, kraft cellulose, soda-AQ cellulose, kraft lignin, and soda-AQ lignin) sere collected at the exit of the Laboratory-scale pyrolysis reactor in fritted glass TD tubes (Supelco, Bellefonte, PA; O.D.: 6.35 mm; length: 88.9 mm) for 15 s. These tubes contained 100 mg of Tenax® TA (80–100 mesh purchased from Supelco, Bellefonte, PA) packed in synthesized glass wool layers. After collecting samples in TD tubes, the analysis was performed using TD/GC–MS. Therma desorption (TD) was employed to release the volatile compounds captured by the sorbent material in the tubes, facilitating their identification and quantification on the GC/MS. TD was carried out using a thermal desorption system

unit (TD-20, Shimadzu, Japan) equipped with an HP-5 MS column (column length: 60 m, inner diameter: 0.25 mm, film thickness: 0.25 μm, J&W Scientific, Agilent Technologies, Santa Clara, California, USA), involving two steps: tube desorption and trap desorption. The mass spectrometer operated in scan mode (41–450 m/z), and volatile organic compounds were identified by comparing their mass spectra with those in the NIST11 library database, using 1-bromo-3-chlorobenzene as an internal standard (Fig. 1).

3. Results and discussion

3.1. Cold alkaline extraction (CAE)

Cold alkaline extractions were utilized to extract hemicelluloses in a liquid medium. The extraction process resulted in solid rich in cellulose and lignin after the removal of hemicelluloses. In Table 3, the main components of the solid residue following hemicellulose extraction from the selected raw materials are shown. The hemicellulose yields are referred to as the quantity of dry hemicellulose obtained relative to the quantity of raw material introduced in the cold alkaline extraction process.

The yield of hemicellulose obtained from Poplar after cold alkaline extraction is less than 5 % as shown in Table 3. This is mainly attributed to the structural characteristics of Poplar which make the alkaline liquor difficult to penetrate and act on, resulting in a low yield of hemicellulose. Hemicellulose yield is directly related to cold alkaline extraction process yield. It has been observed that woody materials exhibit lower extraction yields compared to herbaceous materials, as demonstrated by various studies. For instance, Carvalho et al. 2016 [21] achieved extraction yields of 4.52 % and 37.7 % from eucalyptus and straw, respectively. The composition of obtained solid in the cold alkaline extraction process from Tagasaste was found to be intermediate between those of Poplar and Wheat Straw, containing significant amounts of glucan and xylan. This extraction treatment is selective for the hemicelluloses but does not prevent the extraction of part of the lignin content of the raw material. This means that the extracted hemicellulose fractions are not pure, and their behavior must be further analysed by thermogravimetric analysis.

3.2. Kraft process delignification

Delignification by the kraft process was carried out on the materials studied. The characteristics of the solids obtained are given in Table 4. The yield indicates the amount of pulp produced in relation to the solid obtained from the cold alkaline extraction process; a lower yield means less solid obtained, i.e. a higher extraction in the liquid phase. On the other hand, the kappa index is directly related to the lignin content of the pulp, i.e. the higher the kappa index, the more lignin is found in the pulp and vice versa.

Table 4 shows the characteristics of products obtained through kraft delignification of Poplar, Tagasaste, and Sheat Straw. The yield of the solids obtained from Poplar was the highest at 60.1 %, followed by Tagasaste at 57.84 %, and Wheat Straw at 53.30 %. The Kappa number was highest for Poplar at 16.27, followed by Tagasaste at 14.81 and Wheat Straw at 12.93, indicating that Wheat Straw pulp has the lowest lignin content. The glucan content was highest for Wheat Straw at 78.02 %, followed by Tagasaste at 72.03 % and Poplar at 70.95 %. The xylan content was highest for Poplar at 10.03 %, followed by Tagasaste and Wheat Straw at 8.65 % and 6.24 %, respectively. However, the araban content was highest for Wheat Straw at 1.47 %, followed by Tagasaste at 0.26 % and 0.2 % for Poplar.

The higher extraction observed in agricultural residues, as occurred with Wheat Straw, after kraft treatment results in a lower yield, a phenomenon previously noted by several authors. These results are consistent with those reported in the literature. For instance, in a study involving a simple kraft process, the solid yield for Eucalyptus Citriodora was 47 % with a kappa number of 20.9 [42]. In another study, which focused on optimizing of kraft conditions for wheat straw, the solid yield ranged from 40.02 % to 44.11 %, while the kappa number varied from 18.7 to 47.6 [43].

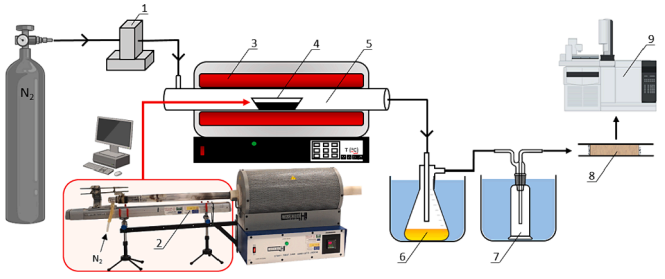

Fig. 1. Schematic of pyrolysis experimental system: (1) Flowmeter, (2) Automatic Sample System, (3) furnace, (4) sample, (5) quartz reaction tube, (6) condenser, (7) cold trap, (8) gas collection (Tenax®), (9) TD-GC/MS.

3.3. Soda-Anthraquinone process delignification

Delignification by the soda-Anthraquinone process was carried out on the materials studied. Table 5 shows the characteristics of the obtained solids in the soda-anthraquinone delignification of Poplar, Tagasaste and Wheat Straw.

The results show that Poplar had the highest yield of 70.89 %, followed by Tagasaste with 65.57 % and Wheat Straw with 60.94 %. Poplar also had the highest kappa number of 42.03, followed by Tagasaste with 33.01 and Wheat Straw with 17.98, in particular the Poplar pulp had 17.73 % of lignin content. The highest glucan content was found in Wheat Straw with 68.02 %, followed by Tagasaste with 64.65 % and Poplar with 58.47 %. The highest xylan content was found in Poplar with 14.17 %, followed by Tagasaste with 11.33 % and Wheat Straw with 9.03 %. The highest araban content was found in Wheat Straw with 2.35 %, followed by Tagasaste with 1.21 % and Poplar with 0.33 %.

Comparing the data presented in Tables 4 and 5, it is clear evident that the pulp yield obtained by soda-anthraquinone delignification exceeds that obtained through kraft delignification. Also, the kappa index obtained with soda-anthraquinone delignification is significantly higher than that obtained with kraft delignification, indicating a greater degree of delignification in kraft process. This difference between the two processes has been observed in various studies, including the work of Alaejos et al. (2006) [44], where the holm yield for kraft and soda-antraquinone processes was reported to be 50.5 % and 55.0 %, respectively, while the corresponding kappa numbers were 20 and 23.7, respectively.

Consequently, the three pulps obtained from different raw material using soda-anthraquinone have slightly less glucan, and more xylan, araban and Klason lignin compared to kraft.

3.4. Thermogravimetric analysis (TGA-DSC)

3.4.1. Raw materials pyrolytic degradation

The TGA and DTG curves shown in Fig. 2 were obtained from Poplar, Tagasaste and Wheat Straw raw materials at a heating rate of 20 °C min^{-1}. The TGA curves show an initial drop, corresponding to the initial peak of the DTG curves, which indicates the loss of moisture from the sample at a temperature of approximately 112 °C for the three raw materials. During this initial phase of dehydration, the sample loses approximately 3.20 % for Poplar, 4.95 % for Tagasaste and 6.01 % for Wheat Straw. This is followed by the active pyrolysis stage (112–500 °C), during which the sample loses most of its weight due to the thermal degradation of the biomass, which is mainly composed of cellulose, hemicellulose, and lignin. The first peak observed in the pyrolysis active region represents the degradation of hemicelluloses and

Table 3
Material balance for the Cold Alkaline Extraction.

	Hemicelluloses Yield (% w/w)[a]	Glucan (% w/w)[b]	Xylan (% w/w)[b]	Araban (% w/w)[b]	Acetyl Groups (% w/w)[b]	Klason Lignin (% w/w)[b]
Poplar	4.59 ± 1.35	45.5 ± 8.25	16.67 ± 1.45	1.24 ± 0.10	2.2 ± 0.01	22.41 ± 4.48
Tagasaste	7.23 ± 2.13	48.18 ± 8.13	14.50 ± 2.60	0.8 ± 0.11	2.65 ± 0.01	21.24 ± 3.76
Wheat Straw	15.52 ± 2.88	49.35 ± 6.18	12.29 ± 0.88	2.61 ± 0.20	2.98 ± 0.01	20.52 ± 1.23

[a] Percentages based on quantity raw material.
[b] Percentages based on obtained solid.

Table 4
Characteristics of solids obtained in kraft delignification.

	Yield Pulp (% w/w)[a]	Kappa Index	Glucan (% w/w)[b]	Xylan (% w/w)[b]	Araban (% w/w)[b]	Klason Lignin (% w/w)[b]
Poplar	60.1 ± 6.84	16.27 ± 3.47	70.95 ± 2.21	10.03 ± 1.05	0.20 ± 0.01	8.34 ± 1.01
Tagasaste	57.84 ± 9.78	14.81 ± 2.02	72.03 ± 2.63	8.65 ± 0.88	0.26 ± 0.05	7.27 ± 0.74
Wheat Straw	53.30 ± 6.82	12.93 ± 1.75	78.02 ± 2.84	6.24 ± 0.62	1.47 ± 0.10	6.56 ± 0.62

[a] Percentages based on solids obtained in CAE.
[b] Percentages based on the kraft pulps obtained.

Table 5
Characteristics of solids obtained in soda-anthraquinone delignification.

	Yield Pulp (% w/w)[a]	Kappa Index	Glucan (% w/w)[b]	Xylan (% w/w)[b]	Araban (% w/w)[b]	Klason Lignin (% w/w)[b]
Poplar	70.89 ± 7.45	42.03 ± 9.58	58.47 ± 5.39	14.17 ± 4.21	0.33 ± 0.07	17.73 ± 4.32
Tagasaste	65.57 ± 9.41	33.01 ± 2.84	64.65 ± 5.96	11.33 ± 2.58	1.21 ± 0.26	15.17 ± 2.15
Wheat Straw	60.94 ± 5.50	17.98 ± 2.05	68.02 ± 7.63	9.03 ± 0.94	2.35 ± 0.46	12.45 ± 1.21

[a] Percentages based on solid obtained in CAE.
[b] Percentages based on solid obtained in soda-anthraquinone process.

lignin. Hemicelluloses start to degrade at around 200 °C and continue to degrade up to around 500 °C due to their relatively low thermal stability [19,34].

After this stage, at around 300 °C, cellulose degradation begins. This follows a similar process to that of hemicellulose, with degradation continuing up to about 600 °C [46]. Lignin, on the other hand, has a more complex structure, which makes it more thermally stable. It undergoes bulk degradation in the temperature range of 150–600 °C [47] and has a lower degradation peak. Therefore, the DTG curve of lignin overlaps with that of hemicelluloses and cellulose. Although cellulose is more thermally stable than hemicellulose, it undergoes degradation in a temperature range of about 390–600 °C due to its crystalline structure. During the active pyrolysis stage, the sample loses 72.17 % of its weight. The final stage of pyrolysis begins at around 500 °C, the passive pyrolysis stage, during which the weight loss of the sample is minimal, and the degradation of lignin is completed.

3.4.2. *Hemicelluloses pyrolytic degradation*

Fig. 3 shows the evolution during pyrolysis (DTG) of hemicelluloses obtained by cold alkaline extraction of the selected raw materials. As can be seen in Fig. 3, both degradation rate of and chemical changes can vary depending on the specific characteristics of the hemicellulose sample being analyzed.

The DTG curves show the three typical phases of hemicellulose degradation. The first phase causes dehydration of the hemicelluloses and results in an average weight loss of 10 % for the three materials. This is mainly due to the moisture remaining in the hemicelluloses after extraction and to the removal of some volatile organic compounds from the hemicellulose. The second phase involves active degradation of the hemicelluloses by pyrolysis (breaking of glycosidic bonds) in the range

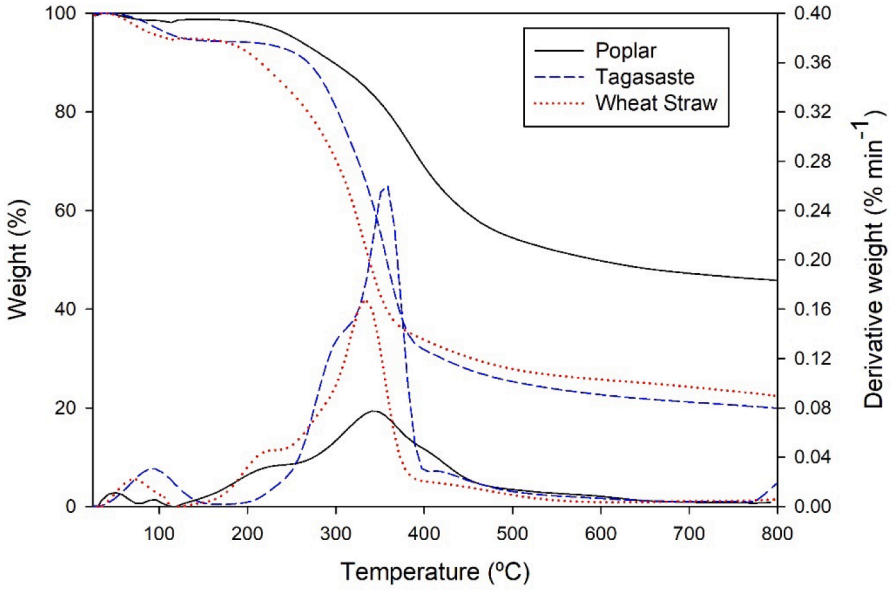

Fig. 2. Pyrolytic evolution (TGA and DTG) curves obtained from Poplar, Tagasaste and Wheat Straw as raw materials under nitrogen atmosphere at 20 °C min^{-1}.

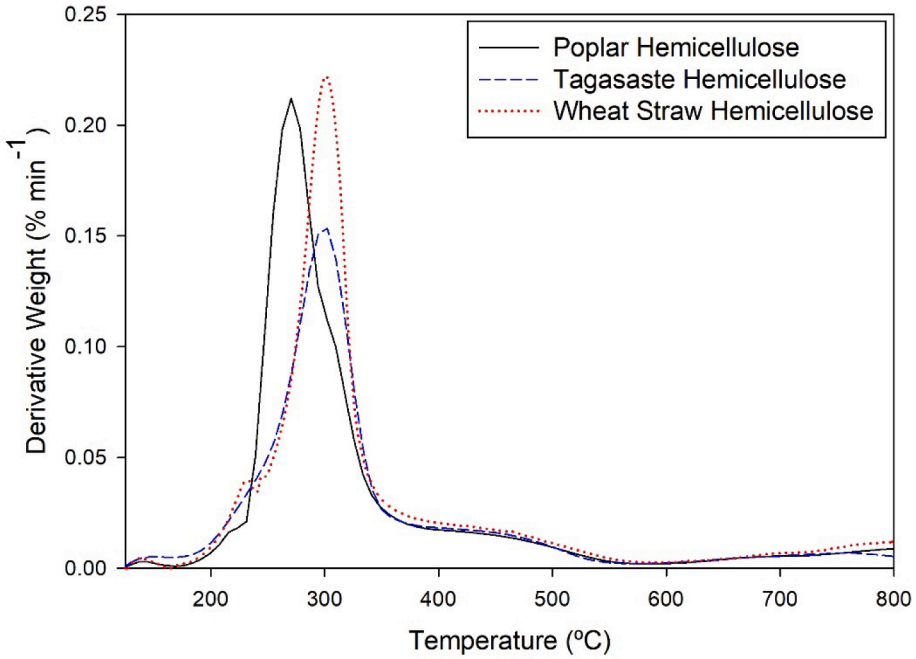

Fig. 3. Pyrolytic evolution (DTG) curves obtained from Poplar, Tagasaste and Wheat Straw extracted hemicelluloses under nitrogen atmosphere at 20 °C min^{-1}.

of 250–350 °C, with a total weight loss of 63.94 %, 42.23 % and 60.27 % for Poplar, Tagasaste and Wheat Straw respectively at 400 °C. The maximum degradation occurs at around 300 °C, mainly due to the depolymerisation of sugars such as xylan, a major component of hemicelluloses [48]. This phase can be further divided into primary and secondary reactions. In the primary reaction, thermal depolymerization of hemicelluloses triggers the production of volatile components such as acetic acid, furfural, and 5-HMF. In the secondary reaction, these volatile compounds further transform into liquid and solid products, such as phenols and aromatics [49]. Finally, the third stage is the passive pyrolysis stage, which occurs at temperatures above 450 °C and involves the transformation of the remaining hemicellulose fragments into a more stable carbonaceous char, through reactions with aromatic compounds and the cracking of carbon-hydrogen and carbon–oxygen bonds [45].

It should be noted that the peaks found in this study for hemicellulose fractions coming from the selected raw materials are smaller than those found in commercial hemicelluloses. This discrepancy could be attributed to the degradation of these linkages during the cold alkaline extraction process, which mainly affects the weaker linkages while preserving the main structure of the hemicelluloses. In addition, commercially available hemicelluloses undergo purification which is not part of the cold alkaline extraction process.

3.4.3. *Celluloses pyrolytic degradation*

The major component of the obtained pulps is cellulose. Fig. 4 shows

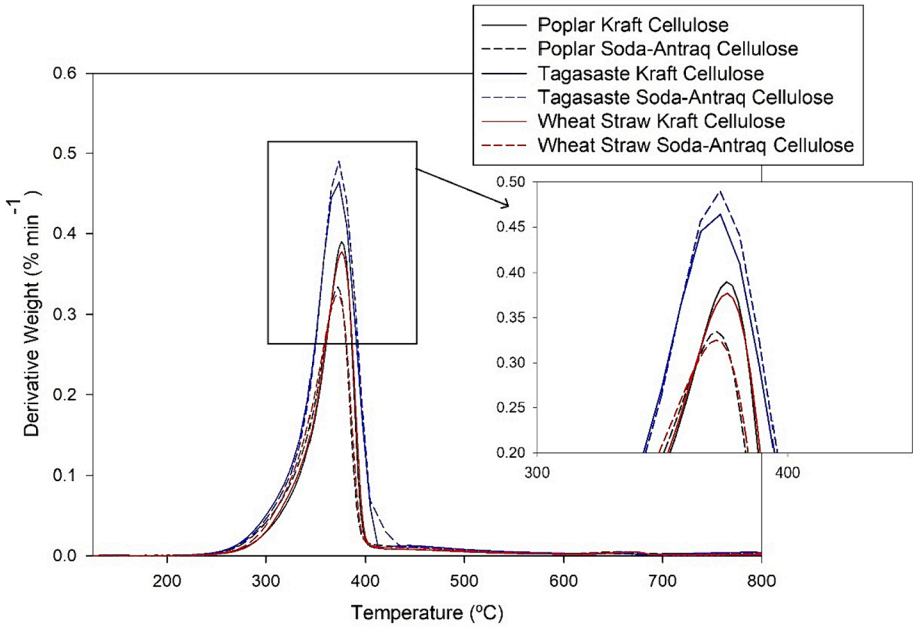

Fig. 4. Pyrolytic evolution (DTG) curves obtained from Poplar, Tagasaste and Wheat Straw kraft and soda-Anthraquinone celluloses under nitrogen atmosphere at 20 °C min^{-1}.

the DTG curves of kraft and soda-anthraquinone pulp for the selected raw materials. Similar to what was found for hemicelluloses, the rate of degradation can also vary depending on the specific characteristics of the cellulose sample being degraded. However, both temperature and degradation intervals appear to be similar between different starting materials and delignification methods. As can be seen, cellulose decomposition occurs in two stages; the first phase takes place at temperatures up to 300 °C and results in the highest weight loss of 80.3 % for all pulps tested. This phase involves the dehydrogenation and decarbonisation of cellulose, leading to the production of levoglucosan, volatile compounds such as levoglucosan (a major product), furans, acetic acid and other oligosaccharides through transglicosilación [50]. Similar to hemicelluloses, the degradation phase of cellulose pyrolysis can be further divided into primary and secondary reactions. The primary reaction involves depolymerisation of the cellulose, releasing volatile organic compounds at the start of the process. The secondary reaction involves the production of liquid and solid products through various chemical reactions in the later stages of the process [16]. The second phase occurs above 500 °C and involves the conversion of volatiles and chars through reactions with aromatics and cracking of the carbon-hydrogen and carbon–oxygen bonds [50]. Both the Kraft and soda-anthraquinone processes exhibit similar cellulose fractions obtained degradation behavior, and both show a single peak representing cellulose degradation, but some differences were observed. For the species studied, the soda-anthraquinone pulps suffers from a higher degradation rate and a higher weight loss compared to those for the kraft process. These differences in the different cellulose fractions contents (Tables 4 and 5) obtained from the different delignification processes may be due to the fact that the soda-anthraquinone process delignifies less due to the lower cellulose content in the final pulp.

3.4.4. *Lignin pyrolytic degradation*

Fig. 5 shows the DTG curves of lignin fractions obtained from the acid hydrolysis of the kraft process and soda-anthraquinone treatment of the selected raw materials. Acid hydrolysis quantitatively extracts Klason lignin, which is further analyzed. A similar evolution to those found for hemicellulose and cellulose has been found for lignin. Also the degradation intervals of lignin pyrolysis can vary depending on factors such as the source of lignin and the delignification method. Lignin is a very complex and heterogeneous polymer, and its behavior during pyrolysis can be influenced by the presence of other components or by the different specific structures of lignin (depending on the feedstock). In this sense, the temperature ranges for lignin pyrolysis can vary depending on the specific conditions of the delignification process. However, the general temperature range for lignin pyrolysis is between 250 °C and 800 °C [36]. Lignin degradation occurs in a wide temperature range due to its complex structure containing various functional groups connected by strong linear and weak bonds, different degradation maxima are observed in the DTG curves.

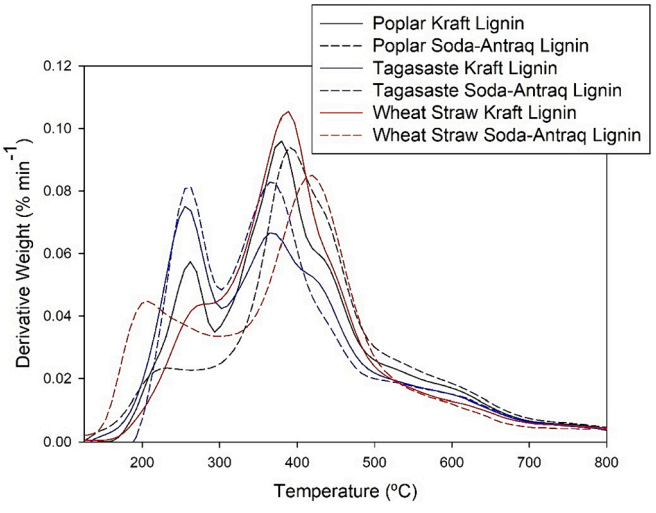

Fig. 5. Pyrolytic evolution (DTG) curves obtained from Poplar, Tagasaste and Wheat Straw Kraft and Soda-Anthraquinone lignins under nitrogen atmosphere at 20 °C min^{-1}.

During lignin pyrolysis, the lignin undergoes three main decomposition phases. The first phase (200–300 °C), shown in Fig. 5, to the degradation of hemicelluloses and celluloses, present as impurities in the lignin due to the delignification process, can be attributed. The second phase (300–500 °C) is the one with the highest rate and weight loss (40.46 % weight loss as an average of the different materials and treatments), which is attributed to the degradation of β-O-4 alkyl-aryl-ether bonds, resulting in the formation of small molecular weight compounds such as phenolic compounds, such as guaiacol, syringol, and catechol, as well as aromatic hydrocarbons and gasses like carbon dioxide, carbon monoxide, and methane [51]. The third phase (500–800 °C), with a low rate of weight loss (10.15 % weight loss on average for the different materials and treatments), may be due to the degradation of the remaining lignin structures, which undergo thermal cracking to form biochar and a carbon-rich solid residue [52].

Note that, the lignin fractions curves of both processes exhibit noise, which is due to the complexity of reactions and gas flow during the measurement. Comparing the lignin of Wheat Straw from the kraft process to the soda-anthraquinone process reveals differences, including a more reactive sample with a bulk degradation to lower temperatures, and a stronger first stage due to the presence of sulphur in kraft process causing increased rupture of carbon–carbon bonds in lignin. The sample from the soda-anthraquinone process experiences the highest weight loss (39.42 %) in the second stage of pyrolysis.

3.5. *Kinetic analysis.*

Two kinetic models, the Friedman differential, and the Flynn-Wall-Ozawa (FWO) integral, are compared for all samples tested. Figs. 6-8 show the lines obtained in the plot of $\ln(d\alpha/dt)$ vs $1/T$ for the Friedman method and $\ln\beta$ vs $1/T$ for the Flynn-Wall-Ozawa method for all the samples studied. In these figures, the values obtained with the highest (0.90) and lowest (0.10) conversions grade have been excluded because they do not represent the behavior of the sample in the initial and final pyrolysis reactions.

3.5.1. *Hemicelluloses kinetic analysis.*

As can be seen in Fig. 6, the use of both methods has resulted in remarkably high regression coefficients ($R^2 > 0.98$) when analyzing hemicellulose fractions from different sources. Furthermore, it can be concluded that the FWO method gives more favorable results than the Friedman method, as evidenced by the fact that the lines are more parallel when analyzing hemicellulose fractions.

Observing the change in slope in the figures, apart from what is observed in Fig. 3, it is clear that different reactions have taken place during the pyrolytic degradation of hemicelluloses. This is because a change in slope implies a change in activation energy, which in turn implies different reactions involved in the degradation, depending on the conversion degree of the sample. Therefore, by observing this fact in the figures, it is possible to identify the different reactions that have taken place during the pyrolytic degradation of hemicelluloses.

Fig. 7 shows the evolution of the activation energy (obtained from the slope of the calculated regression lines) during the pyrolysis of hemicelluloses obtained by cold alkaline extraction for the three species studied. According to H. Wang et al., (2017) [53], the degradation process of hemicellulose is characterized by a low initial activation energy during the degradation process, which gradually increases as the reaction progresses.

In the samples studied, the calculated activation energy for hemicellulose pyrolysis is in the range of 200–300 kJ mol^{-1}. This value is

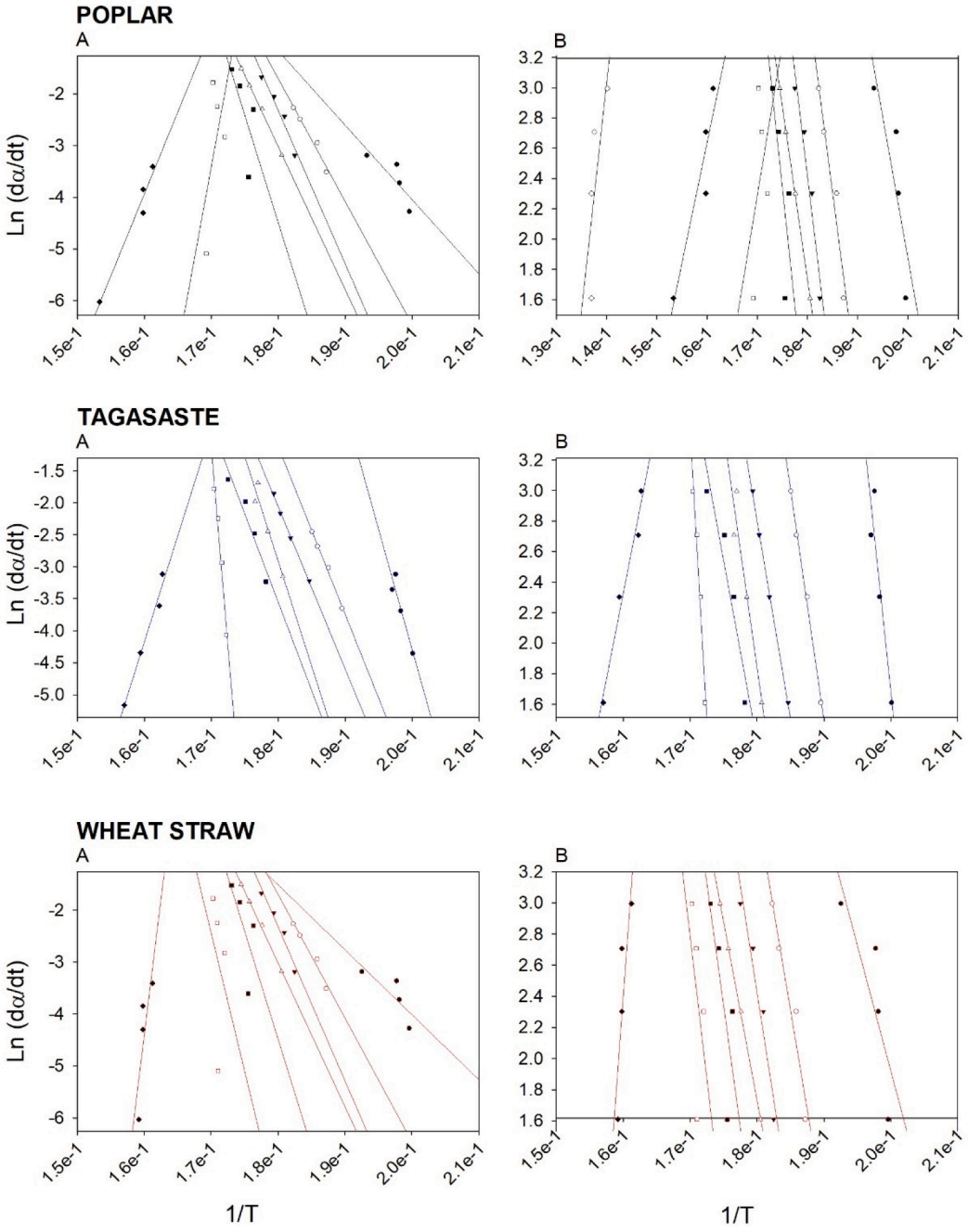

Fig. 6. Evolution of the Friedman (A) and FWO (B) lines for hemicelluloses as a function of the conversion degree (symbols) and the regression lines obtained.

higher than those reported by some authors, which can be attributed to the characteristics of hemicellulose, the method used for its extraction and the type of modelling performed. For instance, in a review of Zhou et al., 2017 [19] the one-reaction/stage models estimated the activation energy of hemicellulose pyrolysis to be in the range of 100–220 kJ mol^{-1}, while the multiple-reaction/stage models estimated the E_a in the range between 26 and 271 kJ mol^{-1}. There are several possible reasons why the activation energy of hemicellulose extracted by cold alkaline extraction is higher than those reported in the literature. Among them, the alkaline extraction method used in the study could result in different chemical structures, properties, and composition of the extracted hemicellulose. For example, the extracted hemicellulose could be contaminated with other compounds, which could affect the pyrolysis behavior and the activation energy. Fig. 2 also suggests that the alkaline extraction method used in the study could result in different chemical structures and properties of the extracted hemicellulose depending on the feedstock.

3.5.2. *Celluloses kinetic analysis.*

Similar to what was observed for hemicelluloses, the use of both methods has resulted in remarkably high regression coefficients ($R^2 >$ 0.99) when analyzing celluloses obtained from different sources and processes. The high R^2 values obtained with both methods indicate that they are reliable in predicting the pyrolysis behavior of cellulose and can be used to estimate the activation energy of cellulose pyrolysis. In addition, based on the high calculated regression coefficients, it is found that the pyrolysis of cellulose follows first order reaction kinetics, as stated by H. Fan et al., 2022 [54].Furthermore, similar to what was found for hemicelluloses, it can be inferred that the FWO method gives more favorable results (higher R^2) than the Friedman method also for

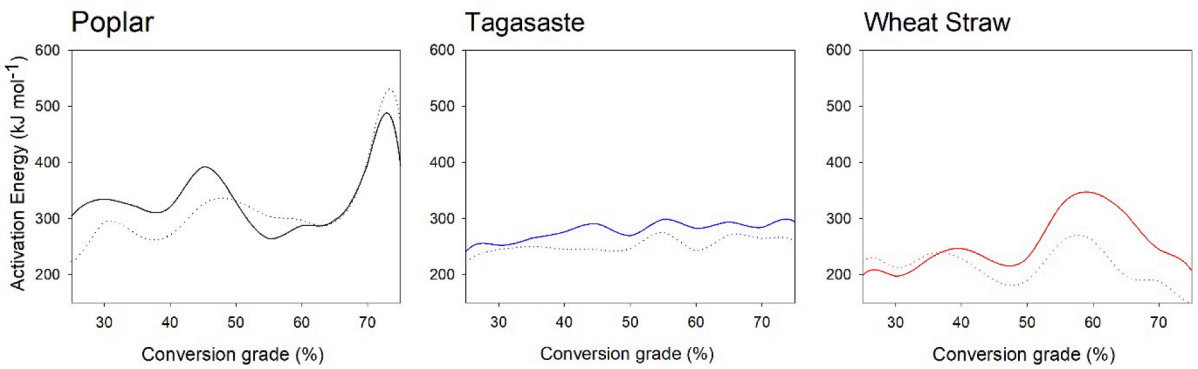

Fig. 7. Activation Energy evolution for extracted hemicelluloses. Continuous lines for Friedman method and discontinuous lines for FWO method.

celluloses [48,55]. This suggests that the FWO method is more accurate in predicting the pyrolysis behavior of cellulose than the Friedman method.

In Fig. 8, a similar slope for almost all measured reaction degrees can be observed. This may be attributed to the high purity of cellulose extracted using both studied delignification methods. In this case, the Friedman method shows a closer resemblance in slope compared to the Flynn method.

Fig. 9 illustrates the evolution of activation energy during the pyrolysis of the obtained celluloses. This figure shows that the activation energy increases as the reaction degree increases, which is in agreement with the literature.

For the cases studied, the values calculated by the FWO method are always higher than those found by the Friedman method. Moreover, the calculated values by the FWO method (180–220 kJ mol^{-1}) are within the range calculated by other authors.

In this sense, the activation energy of cellulose pyrolysis has been reported to be in the range of 114–288 kJ mol^{-1} [50,56,57]. The average pyrolysis activation energy of cellulose has been reported to be 189.2 kJ mol^{-1}[16]. Therefore, it is important to consider the experimental conditions and the method used when comparing the activation energy values reported in different studies.

3.5.3. *Lignins kinetic analysis.*

Fig. 10 presents an insightful analysis of the kinetic evolution of lignin, utilizing both the Friedman and FWO methods.

According to the studies conducted by L. Luo et al., 2020 and Matusiak et al., 2020 [57,58], the activation energies obtained through both methods do not demonstrate a clear linear trend with lignin content as the degree of reaction progresses. This observation can be attributed to the intricate nature of lignin decomposition, which involves multiple reactions with varying activation energies due to the diverse range of bonds and the multi-phasic character of its conversion Radojević et al., 2018 [59]. This complexity is reflected in Fig. 10 through the different slopes depicted.

Fig. 11 illustrates the evolution of activation energy during the pyrolysis of the obtained lignins.

Fig. 11 shows that the activation energy required to break chemical bonds in lignin is higher than that for cellulose. It should be noted that similar values of activation energy were found between the two kinetic models for the different lignins under investigation. According to L. Li, et al., 2013 and L. Luo et al., 2020 [60,57], the results show that the activation energy of lignin increases as the conversion degree progresses, indicating a higher energy requirement to break lignin bonds. This observation holds true for all three species and the two delignification methods investigated in the study. The increase in activation energy can be attributed to several factors. First, as lignin is depolymerised, the larger lignin molecules exhibit increased resistance to pyrolytic degradation. Secondly, the pyrolysis of lignin involves a complex interplay of reactions including fragmentation, condensation, and recombination. As the pyrolysis reaction progresses, the composition of the reaction mixture changes, leading to the dominance of different reaction pathways [61].

It should be noted that the evolution of the activation energy during the pyrolysis of the different lignins studied is different, since this evolution can be influenced by several factors, including the origin and composition of the lignin and the delignification method used. Different chemical compositions and structures of lignin, resulting in variations in pyrolysis kinetics and activation energy profiles, according to the literature cited.

In this case, the Fig. 11 shows that the delignification method has a strong influence on the activation energy, more so than the hemicelluloses and celluloses present in the lignin samples. The literature indicates that lignin has relatively high activation energy values [58], which range from 126 to 200 kJ mol^{-1}, depending on the study and the method used to estimate it [54,62,63].

3.6. *Obtained gasses by pyrolysis from different fractions*

It's essential to emphasize that temperature ranges and the composition of evolved gasses during the pyrolysis of the different lignocellulosic biomass fractions may exhibit variations influenced by factors such as the source plant, experimental conditions, and heating rate [64,65].

Fig. 12 shows the families of compounds detected during the pyrolysis of the different fraction. These gas streams have the potential for uses as fuel. Currently, there is a growing interest in selectively separating these compounds for specific applications [66]. For instance, among the compounds detected was acetic acid, which can be utilized as a platform chemical for the productions of different chemicals and materials [60]. Furthermore, apart from these non-condensable gases, a substantial amount of lighter gases, such as carbon dioxide, hydrogen, carbon monoxide, and methane, have been reported by other authors [65,67,68].

One family of compounds commonly associated whit the hemicellulose and cellulose degradation are furans, with hemicellulose being more prone to their formation, as observed in Fig. 12. Poplar wood and Wheat Straw primarily yielded fundamentally esters (28.9 % and 31.1 %, respectively), furans (20.2 % and 22.6 %, respectively), and aromatic hydrocarbons (16 % and 21.7 %, respectively). In contrast, Tagasaste predominantly produced aldehydes (32.4 %), carboxylic acid (13 %), and furans (11.9 %). The variation observed can be attributed to the inherent properties of the raw materials. This is due to the fact that the composition and the degree of acetylation of the hemicelluloses are dependent on the raw material used. For instance, the divergence stems from the differing sugar monomers present in the raw materials, which decompose at different temperatures and produce different gas products. Hardwoods contain predominantly xylose, whereas softwoods

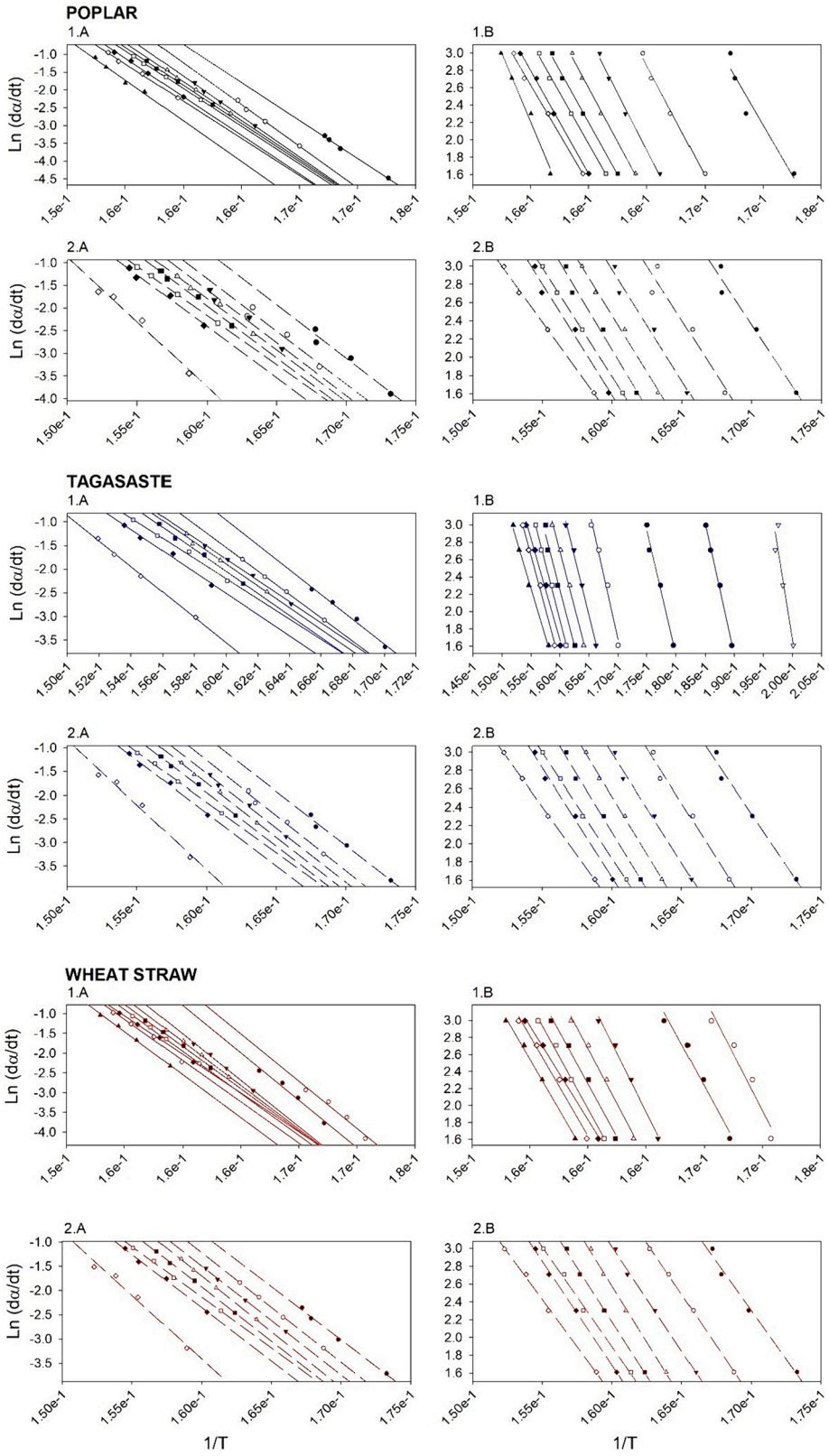

Fig. 8. Evolution of the Friedman (A) and FWO (B) lines for Kraft (1) and Soda-Antraquinone (2) celluloses as a function of the conversion degree (symbols) and the regression lines obtained.

contain a combination of xylose, mannose, and galactose [69,70]. If we refer back to the DTG-curve of hemicellulose fractions (Fig. 3), we can observe a difference in the degradation of Tagasaste's hemicellulose fractions compared to that found for Poplar and Wheat Straw.

Focusing on the cellulose fractions, it is observed in the gas stream produced during pyrolysis that the most prominent compounds are aldehydes, and phenols, while in the Poplar case by the second one, the carboxylic acids. Therefore, as mentioned above, the production of

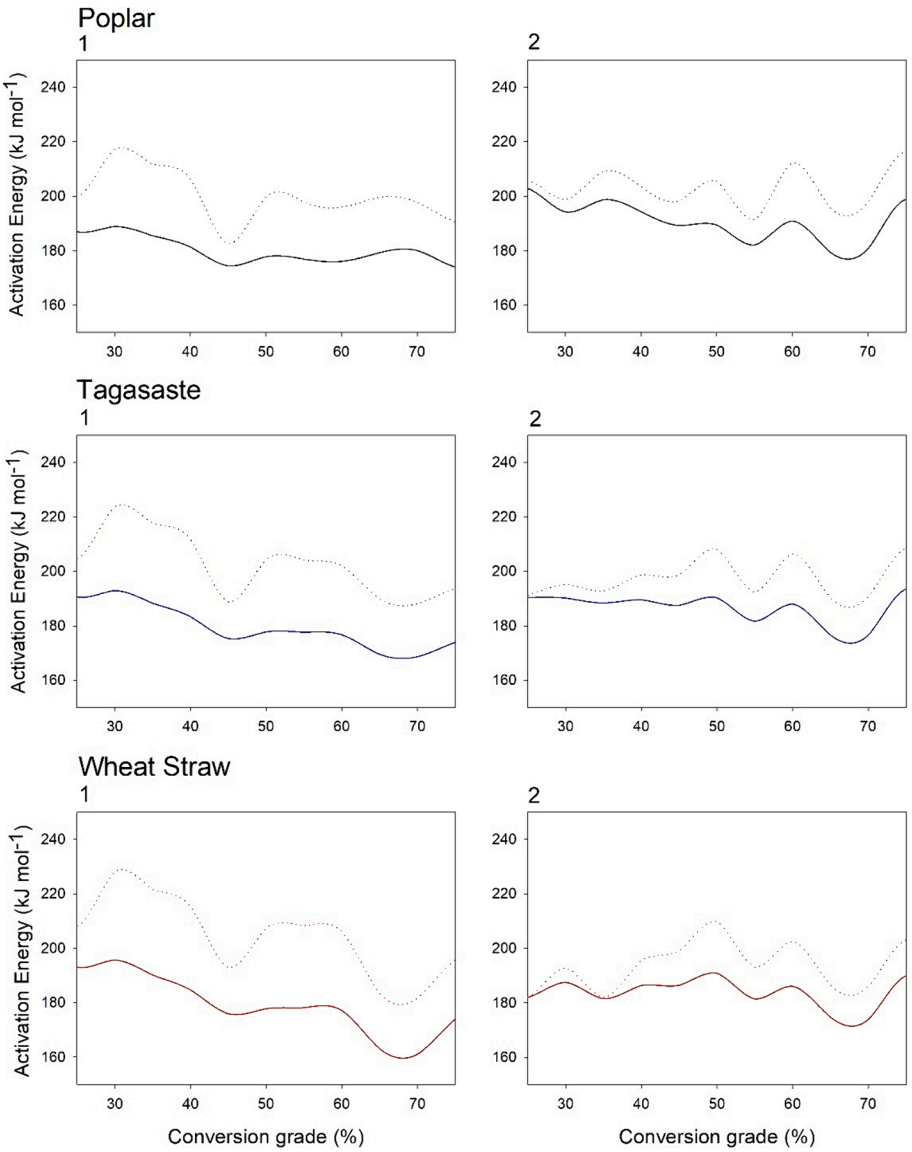

Fig. 9. Activation Energy evolution for kraft (1) and Soda-Antraquinone (2) celluloses by Friedman (continuous lines) and FWO (discontinuous lines) methods.

specific compounds and their amounts depend on the initial raw material. With regard to the cellulose fraction, the crystallinity and degree of polymerization vary among different feedstocks. For example, softwoods generally have a higher crystallinity than hardwoods and agricultural residues [71–73]. Sun et al., 2022 [74] reported that cellulose pyrolysis produces aldehydes, acids, alcohols, ketones, carbohydrates, and other. In Poplar, a significant amount of the aldehyde prop-2-enal (29.5 %) was identified, while the primary aldehyde in the cellulose fractions of Tagasaste and Wheat Straw was 3-Methylbutanal (14.2 % and 18.1 %, respectively).

Regarding the lignin fractions, the differences between Tagasaste, Poplar and Wheat Straw are similar to those observed in the hemicellulose fractions. In this case, the most abundant family of compounds obtained from Poplar and Wheat Straw was aromatic hydrocarbons, predominantly toluene (40.8 % and 31.6 %, respectively). However, in Tagasaste's lignin fraction, the predominant group of compounds were phenols (28.2 %). For this fraction, there is also a correlation between the feedstock and the pyrolytic gases, as the lignin composition is also influenced by the feedstock's composition. Specifically, softwoods have a higher lignin content with a predominantly guaiacyl units, whereas hardwoods contain a higher proportion of syringyl units [75].

One compound deserving special mention is furfural, which has been recognized as one of the top biomass-derived platform compounds by the US Department of Energy [76]. Furfural has the potential to yield high-value products, including liquid hydrocarbon fuels, fuel additives, and furfural derivatives with various applications [77,78]. In summary, the furfural serves as a valuable source of derivatives that have the potential to become biofuel components [79]. In this work, we observed that pyrolysis produced a significant quantity of furans, especially furfural, primarily originating from hemicellulose fractions. Wheat Straw exhibited the highest furfural production, accounting for 19.3 %, followed by Poplar with 16.9 %, and Tagasaste with the lowest at 6.6 %.

4. Conclusions

The thermogravimetric analysis revealed similar degradation patterns across the studied raw materials (Poplar, Tagasaste, and Wheat Straw), with distinct characteristics for each lignocellulosic fraction. Cellulose exhibited a single peak around 370 °C, hemicellulose degraded earlier (250 – 300 °C) with a smoother profile, and lignin showed a broader range (15 – 600 °C) that is less prevalent in raw materials due to overlapping degradation with other components. The activation energy (E_a) required for degradation varied depending on the fraction and conversion degree, with hemicellulose (200–300 kJ mol^{-1}) requiring

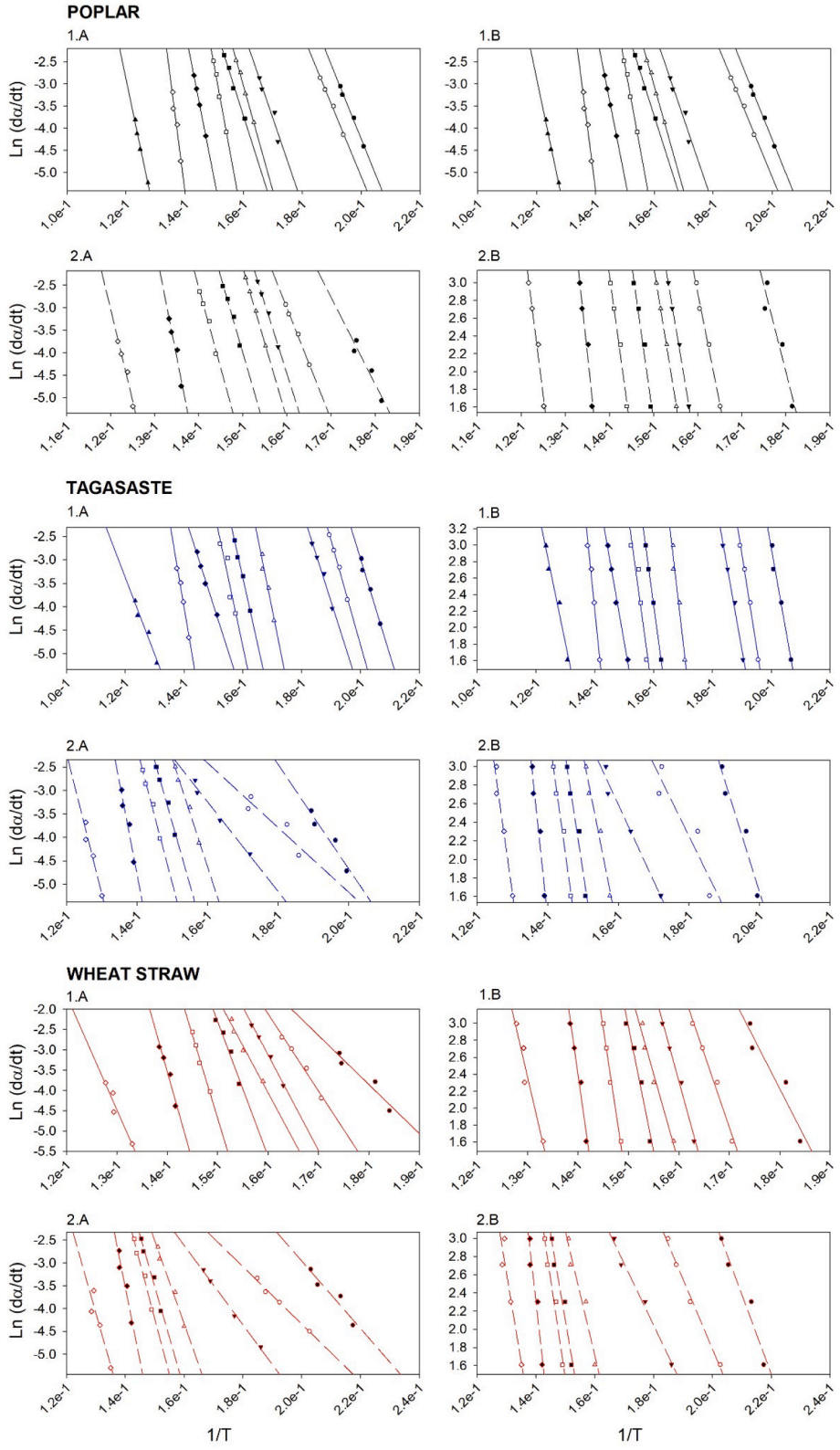

Fig. 10. Evolution of the Friedman (A) and FWO (B) lines for kraft (1) and Soda-Antraquinone (2) lignins as a function of the conversion degree (symbols) and the regression lines obtained.

slightly higher E_a than cellulose (180–220 kJ mol^{-1}). Lignin fractions displayed the highest E_a; variations exist among different lignins, influenced by factors such as the origin of the raw material and the delignification method employed to obtain the lignin fraction. The pyrolysis process generated a diverse gas stream, with a wide range of components, originating from different lignocellulosic fractions. Highlighting the presence of furfural, more pronounced in the pyrolysis of hemicellulose fractions, especially in hemicellulose obtained from Wheat Straw. This observation underscores a potential avenue for the targeted production of high-value-added chemicals from specific

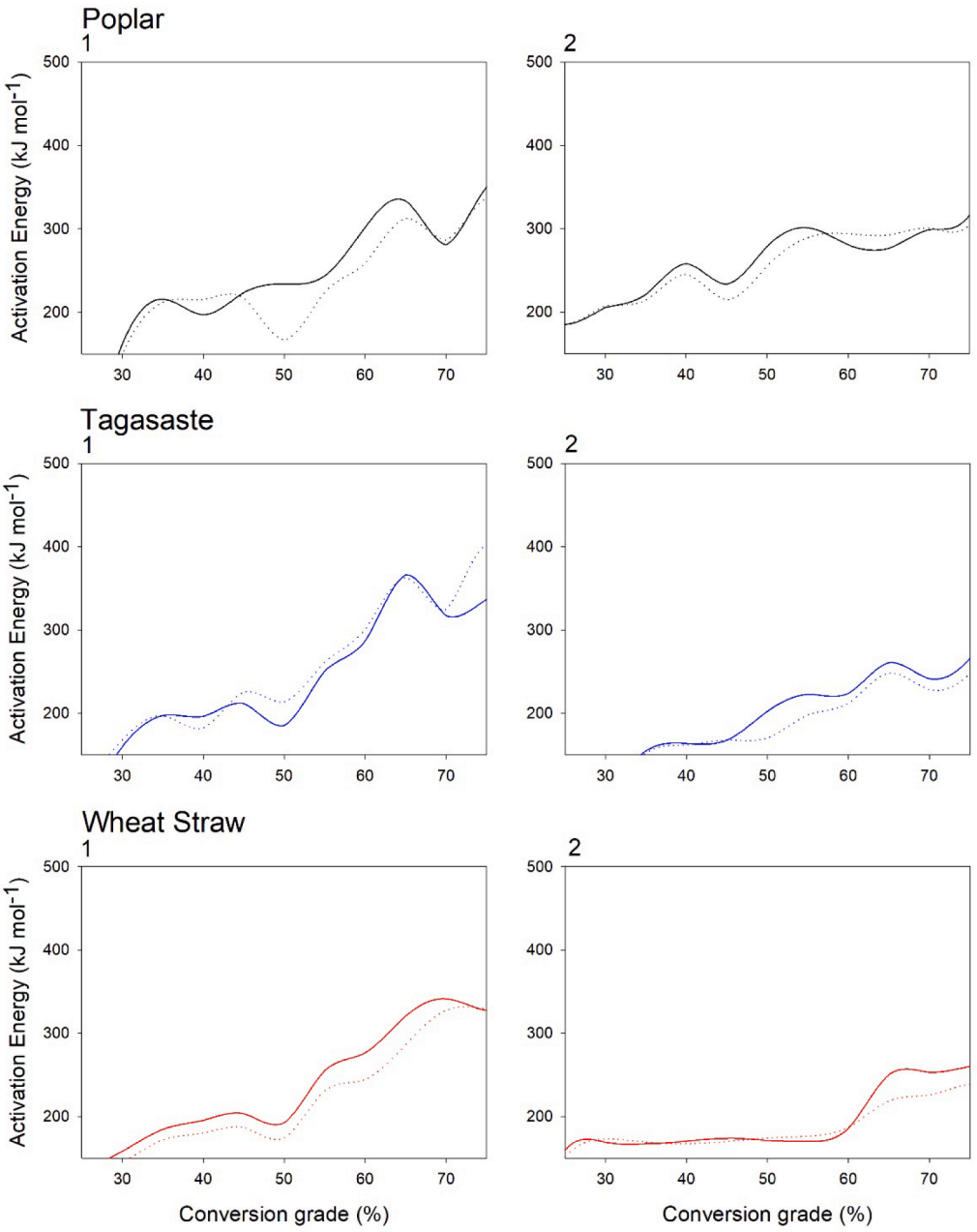

Fig. 11. Activation Energy evolution for kraft (1) and Soda-Antraquinone (2) lignins by Friedman (continuous lines) and FWO (discontinuous lines) methods.

biomass sources.

Ethics approval and consent to participate

The authors declare that this is their original work, and the corresponding manuscript has not been published before and is only submitted to Fuel.

Consent for publication

All authors reviewed the manuscript and consented to its publication.

Availability of data and materials

All data generated or analyzed during this work are included in this published article.

Funding

This study was supported by the Ministry of Science and Innovation (Spain), as well as by the National Research Program Oriented to the Challenges of Society (Project PID2020-112875RB-C21 funded by MCIN/AEI /https://doi.org/10.13039/501100011033), also this publication is part of the PRE2021-097925 support (funded by MCIN/AEI/ https://doi.org/10.13039/501100011033 and by the FSE+). Funding for open access charge: Universidad de Huelva/CBUA.

CRediT authorship contribution statement

N. Almagro-Herrera: Visualization, Methodology, Investigation, Formal analysis, Data curation, Conceptualization. **S. Lozano-Calvo:** Writing – original draft, Visualization, Methodology, Investigation, Formal analysis, Data curation, Conceptualization. **A. Palma:** Writing – review & editing, Visualization, Methodology, Investigation, Formal analysis, Data curation, Conceptualization. **J.C. García:** Conceptualization, Methodology, Funding acquisition, Supervision, Project administration. **M.J. Díaz:** Conceptualization, Methodology, Formal analysis, Data curation, Funding acquisition, Supervision, Writing – review & editing, Project administration.

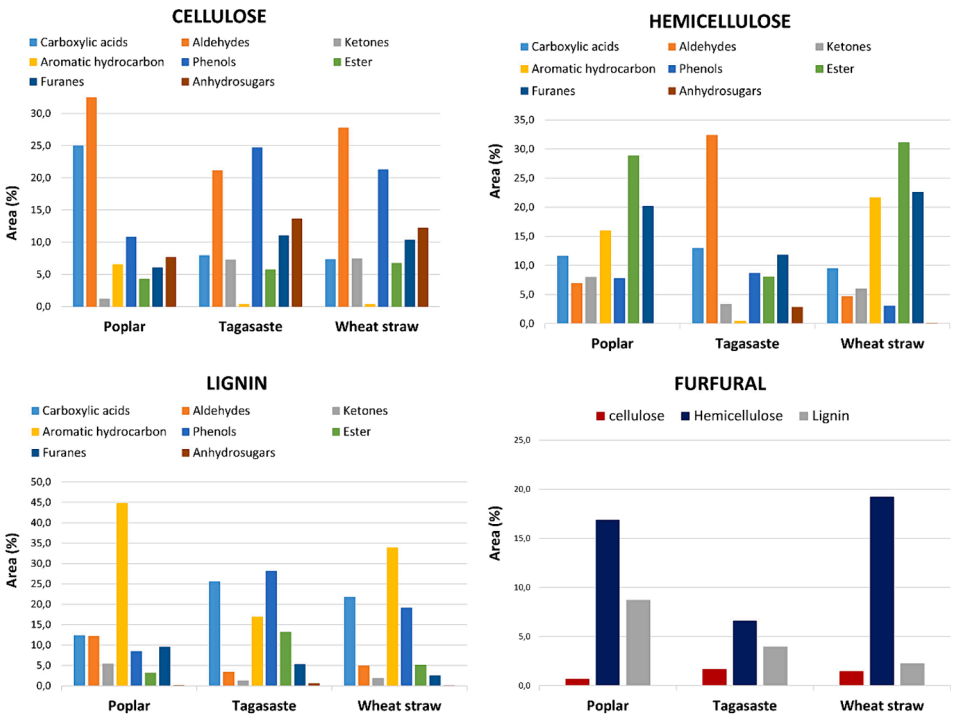

Fig. 12. Pyrolysis-gas products (% area) of the different fractions (cellulose, hemicellulose, and lignin) of Poplar, Tagasaste and Wheat Straw, and furfural production from the different fractions.

Declaration of competing interest

The authors declare that they have no known competing financial interests or personal relationships that could have appeared to influence the work reported in this paper.

Data availability

All data generated or analyzed during this work are included in this published article.

References

[1] Alper K, Tekin K, Karagöz S, Ragauskas AJ. Sustainable energy and fuels from biomass: a review focusing on hydrothermal biomass processing. Sustain Energy Fuels 2020;4:4390–414. https://doi.org/10.1039/D0SE00784F.

[2] Roy P, Jahromi H, Rahman T, Baltrusaitis J, Hassan EB, Torbert A, et al. Hydrotreatment of pyrolysis bio-oil with non-edible carinata oil and poultry fat for producing transportation fuels. Fuel Process Technol 2023;245:107753. https://doi.org/10.1016/J.FUPROC.2023.107753.

[3] Sharma V, Tsai ML, Nargotra P, Chen CW, Sun PP, Singhania RR, et al. Journey of lignin from a roadblock to bridge for lignocellulose biorefineries: a comprehensive review. Sci Total Environ 2023;861:160560. https://doi.org/10.1016/J.SCITOTENV.2022.160560.

[4] Ayub Y, Zhou J, Shi T, Ren J. Process safety assessment of thermal technologies for biomass valorization by numerical descriptive approach. Process Saf Environ Prot 2023;171:803–11. https://doi.org/10.1016/J.PSEP.2023.01.075.

[5] Troiano DT, Hofmann T, Brethauer S, Studer MHP. Toward optimal use of biomass as carbon source for chemical bioproduction. Curr Opin Biotechnol 2023;81:102942. https://doi.org/10.1016/J.COPBIO.2023.102942.

[6] Akram HA, Imran M, Javaid A, Latif S, Rizvi NB, Jesionowski T, et al. Pretreatment and catalytic conversion of lignocellulosic and algal biomass into biofuels by metal organic frameworks. Mol Catal 2023;539:112893. https://doi.org/10.1016/J.MCAT.2022.112893.

[7] Zhan Q, Lin Q, Wu Y, Liu Y, Wang X, Ren J. A fractionation strategy of cellulose, hemicellulose, and lignin from wheat straw via the biphasic pretreatment for biomass valorization. Bioresour Technol 2023;376:128887. https://doi.org/10.1016/J.BIORTECH.2023.128887.

[8] Fan Q, Fu P, Song C, Fan Y. Valorization of waste biomass through hydrothermal liquefaction: a review with focus on linking hydrothermal factors to products characteristics. Ind Crops Prod 2023;191:116017. https://doi.org/10.1016/J.INDCROP.2022.116017.

[9] Mujtaba M, Fraceto L, Fazeli M, Mukherjee S, Savassa SM, Araujo de Medeiros G, et al. Lignocellulosic biomass from agricultural waste to the circular economy: a review with focus on biofuels, biocomposites and bioplastics. J Clean Prod 2023;402:136815. https://doi.org/10.1016/J.JCLEPRO.2023.136815.

[10] Amenaghawon AN, Anyalewechi CL, Okieimen CO, Kusuma HS. Biomass pyrolysis technologies for value-added products: a state-of-the-art review. Environ Dev Sustain 2021;23:14324–78. https://doi.org/10.1007/s10668-021-01276-5.

[11] Vuppaladadiyam AK, Vuppaladadiyam SSV, Sahoo A, Murugavelh S, Anthony E, Bhashkar T, et al. Bio-oil and biochar from the pyrolytic conversion of biomass: a current and future perspective on the trade-off between economic, environmental, and technical indicators. Sci Total Environ 2023;857:159155. https://doi.org/10.1016/J.SCITOTENV.2022.159155.

[12] Okolie JA, Epelle EI, Tabat ME, Orivri U, Amenaghawon AN, Okoye PU, et al. Waste biomass valorization for the production of biofuels and value-added products: a comprehensive review of thermochemical, biological and integrated processes. Process Saf Environ Prot 2022;159:323–44. https://doi.org/10.1016/J.PSEP.2021.12.049.

[13] Eugenio ME, Ruiz-Montoya M, Martín-Sampedro R, Ibarra D, Díaz MJ. Influence of cellulose Characteristics on pyrolysis suitability. Processes 2021;9. https://doi.org/10.3390/pr9091584.

[14] Madanayake BN, Gan S, Eastwick C, Ng HK. Biomass as an energy source in coal co-firing and its feasibility enhancement via pre-treatment techniques. Fuel Process Technol 2017;159:287–305. https://doi.org/10.1016/J.FUPROC.2017.01.029.

[15] Wu W, Mei Y, Zhang L, Liu R, Cai J. Effective activation energies of lignocellulosic biomass pyrolysis. Energy Fuel 2014;28:3916–23. https://doi.org/10.1021/ef5005896.

[16] Chen D, Cen K, Zhuang X, Gan Z, Zhou J, Zhang Y, et al. Insight into biomass pyrolysis mechanism based on cellulose, hemicellulose, and lignin: evolution of volatiles and kinetics, elucidation of reaction pathways, and characterization of gas, biochar and bio-oil. Combust Flame 2022;242:112142. https://doi.org/10.1016/J.COMBUSTFLAME.2022.112142.

[17] Al-Rumaihi A, Shahbaz M, Mckay G, Mackey H, Al-Ansari T. A review of pyrolysis technologies and feedstock: a blending approach for plastic and biomass towards optimum biochar yield. Renew Sustain Energy Rev 2022;167:112715. https://doi.org/10.1016/J.RSER.2022.112715.

[18] Stefanidis SD, Kalogiannis KG, Iliopoulou EF, Michailof CM, Pilavachi PA, Lappas AA. A study of lignocellulosic biomass pyrolysis via the pyrolysis of cellulose, hemicellulose and lignin. J Anal Appl Pyrolysis 2014;105:143–50. https://doi.org/10.1016/J.JAAP.2013.10.013.

[19] Zhou X, Li W, Mabon R, Broadbelt LJ. A critical review on hemicellulose pyrolysis. Energ Technol 2017;5:52–79. https://doi.org/10.1002/ente.201600327.

[20] Carrier M, Windt M, Ziegler B, Appelt J, Saake B, Meier D, et al. Quantitative insights into the fast pyrolysis of Extracted cellulose, hemicelluloses, and lignin. ChemSusChem 2017;10:3212–24. https://doi.org/10.1002/cssc.201700984.

[21] de Carvalho DM, Sevastyanova O, de Queiroz JH, Colodette JL. Cold alkaline extraction as a pretreatment for bioethanol production from eucalyptus, sugarcane bagasse and sugarcane straw. Energy Convers Manag 2016;124:315–24. https://doi.org/10.1016/j.enconman.2016.07.029.

[22] Hult E-L, Larsson PT, Iversen T. A comparative CP/MAS 13C-NMR study of cellulose structure in spruce wood and kraft pulp. Cellul 2000;7:35–55.

[23] Newman RH, Hemmingson JA, Suckling ID. Carbon-13 nuclear magnetic resonance studies of kraft pulping; 1993.
[24] Gustafson RR, Sleicher CA, McKean WT, Finlayson BA. Theoretical model of the kraft pulping process. Ind Eng Chem Process Des Dev 1983;22:87–96.
[25] Martínez JM, Reguant J, Salvadó J, Farriol X. Soda-anthraquinone pulping of a softwood mixture: applying a pseudo-kinetic severity parameter. Bioresour Technol 1997;60:161–7.
[26] Rabemanolontsoa H, Saka S. Various pretreatments of lignocellulosics. Bioresour Technol 2016;199:83–91. https://doi.org/10.1016/J.BIORTECH.2015.08.029.
[27] García JC, Díaz MJ, Garcia MT, Feria MJ, Gómez DM, López F. Search for optimum conditions of wheat straw hemicelluloses cold alkaline extraction process. Biochem Eng J 2013;71:127–33. https://doi.org/10.1016/j.bej.2012.12.008.
[28] Park YC, Kim JS. Comparison of various alkaline pretreatment methods of lignocellulosic biomass. Energy 2012;47:31–5. https://doi.org/10.1016/j.energy.2012.08.010.
[29] Lozano Calvo S. Extracción de Polisacáridos en Especies de Alta Productividad Aplicando Ultrasonidos. Huelva: 2019.
[30] TAPPI T264 cm-07. Preparation of wood for chemical analysis.TAPPI Press, Atlanta, GA. 2007.
[31] Pola L, Collado S, Oulego P, Díaz M. Kraft black liquor as a renewable source of value-added chemicals. Chem Eng J 2022;448:137728. https://doi.org/10.1016/J.CEJ.2022.137728.
[32] López F, Trinidad García M, Mena V, Loaiza JM, Zamudio MAM, García JC. Can acceptable pulp be obtained from Eucalyptus globulus wood chips after hemicellulose extraction? vol. 10. 2015.
[33] TAPPI T204 cm-07. Solvent extractives of wood and pulp. TAPPI Press, Atlanta, GA. 2007.
[34] TAPPI T222 om-11. Acid-insoluble lignin in wood and pulp. TAPPI Press, Atlanta, GA. 2011.
[35] TAPPI T249 cm-09. Carbohydrate composition of extractive-free wood and wood pulp by gas-liquid chromatography. TAPPI Press, Atlanta, GA. 2009.
[36] Van de Velden M, Baeyens J, Brems A, Janssens B, Dewil R. Fundamentals, kinetics and endothermicity of the biomass pyrolysis reaction. Renew Energy 2010;35:232–42. https://doi.org/10.1016/J.RENENE.2009.04.019.
[37] Siddiqi H, Bal M, Kumari U, Meikap BC. In-depth physiochemical characterization and detailed thermo-kinetic study of biomass wastes to analyze its energy potential. Renew Energy 2020;148:756–71. https://doi.org/10.1016/J.RENENE.2019.10.162.
[38] Ozawa T. A new method of analyzing thermogravimetric data. Bull Chem Soc Jpn 1965;38:1881–6. https://doi.org/10.1246/bcsj.38.1881.
[39] Flynn JH, Wall LA. A quick, direct method for the determination of activation energy from thermogravimetric data. J Polym Sci B 1966;4:323–8. https://doi.org/10.1002/pol.1966.110040504.
[40] Venkatesh M, Ravi P, Tewari SP. Isoconversional kinetic analysis of decomposition of nitroimidazoles: friedman method vs Flynn–Wall–Ozawa method. J Phys Chem A 2013;117:10162–9. https://doi.org/10.1021/jp407526r.
[41] Friedman HL. Kinetics of thermal degradation of char-forming plastics from thermogravimetry. application to a phenolic plastic. J Polym Sci Part C: Polym Symposia Wiley Online Library 1964;6:183–95.
[42] Khristova P, Kordsachia O, Patt R, Dafaalla S. Alkaline pulping of some eucalypts from Sudan. Bioresour Technol 2006;97:535–44. https://doi.org/10.1016/J.BIORTECH.2005.04.006.
[43] Deniz I, Kirci H, Ates S. Optimisation of wheat straw Triticum drum kraft pulping. Ind Crops Prod 2004;19:237–43. https://doi.org/10.1016/J.INDCROP.2003.10.011.
[44] Alaejos J, López F, Eugenio ME, Tapias R. Soda–anthraquinone, kraft and organosolv pulping of holm oak trimmings. Bioresour Technol 2006;97:2110–6. https://doi.org/10.1016/J.BIORTECH.2005.09.021.
[45] Ma H, Zhang Y, Wang L, Zhu Z, Chen Y, Wang H, et al. Kinetic Analysis of the Pyrolysis of Apricot Stone and its Main Components via Distributed Activation Energy Mode. vol. 15. 2019.
[46] SriBala G, Vargas DC, Kostetskyy P, de Vijver R, Broadbelt LJ, Marin GB, et al. New perspectives into cellulose fast pyrolysis kinetics using a py-GC × GC-FID/MS system. ACS Engineering Au 2022;2:320–32. https://doi.org/10.1021/acsengineeringau.2c00006.
[47] Domínguez JC, Santos TM, Rigual V, Oliet M, Alonso MV, Rodriguez F. Thermal stability, degradation kinetics, and molecular weight of organosolv lignins from Pinus radiata. Ind Crops Prod 2018;111:889–98. https://doi.org/10.1016/J.INDCROP.2017.10.059.
[48] Yeo JY, Chin BLF, Tan JK, Loh YS. Comparative studies on the pyrolysis of cellulose, hemicellulose, and lignin based on combined kinetics. J Energy Inst 2019;92:27–37. https://doi.org/10.1016/J.JOEI.2017.12.003.
[49] Collard FX, Blin J. A review on pyrolysis of biomass constituents: mechanisms and composition of the products obtained from the conversion of cellulose, hemicelluloses and lignin. Renew Sustain Energy Rev 2014;38:594–608. https://doi.org/10.1016/J.RSER.2014.06.013.
[50] Zhang X, Yang W, Dong C. Levoglucosan formation mechanisms during cellulose pyrolysis. J Anal Appl Pyrolysis 2013;104:19–27. https://doi.org/10.1016/J.JAAP.2013.09.015.
[51] Custodis VBF, Hemberger P, Ma Z, van Bokhoven JA. Mechanism of fast pyrolysis of lignin: studying model compounds. J Phys Chem B 2014;118:8524–31. https://doi.org/10.1021/jp5036579.
[52] Mandlekar N, Cayla A, Rault F, Giraud S, Salaün F, Malucelli G, et al. Thermal stability and fire Retardant properties of polyamide 11 microcomposites containing different lignins. Ind Eng Chem Res 2017;56:13704–14. https://doi.org/10.1021/acs.iecr.7b03085.
[53] Wang H, Yao Q, Wang C, Fan B, Xiong Y, Chen Y, et al. New insight on promoted thermostability of poplar wood modified by MnFe2O4 nanoparticles through the pyrolysis behaviors and kinetic study. Sci Rep 2017;7:1418. https://doi.org/10.1038/s41598-017-01597-4.
[54] Fan H, Gu J, Wang Y, Yuan H, Chen Y. Insight into the pyrolysis kinetics of cellulose, xylan and lignin with the addition of potassium and calcium based on distributed activation energy model. Energy 2022;243:122816. https://doi.org/10.1016/J.ENERGY.2021.122816.
[55] Zhu L, Zhong Z. Effects of cellulose, hemicellulose and lignin on biomass pyrolysis kinetics. Korean J Chem Eng 2020;37:1660–8. https://doi.org/10.1007/s11814-020-0553-y.
[56] Anca-Couce A, Tsekos C, Retschitzegger S, Zimbardi F, Funke A, Banks S, et al. Biomass pyrolysis TGA assessment with an international round robin. Fuel 2020;276:118002. https://doi.org/10.1016/J.FUEL.2020.118002.
[57] Luo L, Guo X, Zhang Z, Chai M, Rahman MM, Zhang X, et al. Insight into pyrolysis kinetics of lignocellulosic biomass: isoconversional kinetic analysis by the modified Friedman method. Energy Fuel 2020;34:4874–81.
[58] Matusiak M, Ślęzak R, Ledakowicz S. Thermogravimetric kinetics of selected energy crops pyrolysis. Energies (Basel) 2020;13. https://doi.org/10.3390/en13153977https://doi.org/10.1021/acs.energyfuels.0c00275.
[59] Radojević M, Janković B, Jovanović V, Stojiljković D, Manić N. Comparative pyrolysis kinetics of various biomasses based on model-free and DAEM approaches improved with numerical optimization procedure. PLoS One 2018;13. https://doi.org/10.1371/journal.pone.0206657.
[60] Li L, Rowbotham JS, Christopher Greenwell H, Dyer PW. An introduction to pyrolysis and catalytic pyrolysis: versatile techniques for biomass conversion. New Future Devel Catal: Catal Biomass Convers 2013:173–208. https://doi.org/10.1016/B978-0-444-53878-9.00009-6.
[61] Wang S, Dai G, Yang H, Luo Z. Lignocellulosic biomass pyrolysis mechanism: a state-of-the-art review. Prog Energy Combust Sci 2017;62:33–86. https://doi.org/10.1016/J.PECS.2017.05.004.
[62] Liu M, Yang J, Liu Z, He W, Liu Q, Li Y, et al. Cleavage of covalent bonds in the pyrolysis of lignin, cellulose, and hemicellulose. Energy Fuel 2015;29:5773–80. https://doi.org/10.1021/acs.energyfuels.5b00983.
[63] Kristanto J, Azis MM, Purwono S. Multi-distribution activation energy model on slow pyrolysis of cellulose and lignin in TGA/DSC. Heliyon 2021;7:e07669.
[64] Carrier M, Fournet R, Sirjean B, Amsbury S, Alfonso YB, Pontalier P-Y, et al. Fast pyrolysis of hemicelluloses into short-chain acids: an investigation on concerted mechanisms. Energy Fuel 2020;34:14232–48. https://doi.org/10.1021/acs.energyfuels.0c02901.
[65] Huang Y, Wang H, Zhang X, Zhang Q, Wang C, Ma L. CO2 pyrolysis kinetics and characteristics of lignin-rich hydrolysis residue produced from a tandem process of steam-stripping and acid hydrolysis. Fuel 2022;316:123361. https://doi.org/10.1016/J.FUEL.2022.123361.
[66] Clemente-Castro S, Palma A, Ruiz-Montoya M, Giráldez I, Díaz MJ. Optimizing pyrolysis parameters and product analysis of a fluidized bed pilot plant for Leucaena leucocephala biomass. Environ Sci Eur 2023;35:88. https://doi.org/10.1186/s12302-023-00800-w.
[67] Pielsticker S, Gövert B, Umeki K, Kneer R. Flash pyrolysis kinetics of Extracted lignocellulosic biomass components. Front Energy Res 2021:9. https://doi.org/10.3389/fenrg.2021.737011.
[68] Li H, Wang L, Ji Y, Xue S, Wang Z. Study on the mechanism of gas component release for biomass pyrolysis. E3S Web of Conferences, vol. 118, EDP Sciences; 2019, p. 03058.
[69] Popa VI, Spiridon J. Hemicelluloses: structure and properties. Polysaccharides: Structural Diversity and Functional Versatility Marcel Dekker, New York 1998:297–311.
[70] Xiao L-P, Song G-Y, Sun R-C. Effect of hydrothermal processing on hemicellulose structure. Hydrothermal processing in biorefineries: production of bioethanol and high added-value compounds of second and third generation biomass 2017:45–94.
[71] Adachi H, Sugiyama J, Kondo Y, Okano T. The difference of cellulose crystal between softwoods and hardwoods. Sen'i Gakkaishi 1991;47:580–4. https://doi.org/10.2115/fiber.47.11_580.
[72] Newman RH. Crystalline forms of cellulose in softwoods and Hardwoods. J Wood Chem Technol 1994;14:451–66. https://doi.org/10.1080/02773819408003107.
[73] Lichtenegger H, Reiterer A, Stanzl-Tschegg SE, Fratzl P. Variation of cellulose microfibril angles in softwoods and Hardwoods—a possible strategy of mechanical optimization. J Struct Biol 1999;128:257–69. https://doi.org/10.1006/JSBI.1999.4194.
[74] Sun T, Zhang L, Yang Y, Li Y, Ren S, Dong L, et al. Fast pyrolysis of cellulose and the effect of a catalyst on product distribution. Int J Environ Res Public Health 2022:19. https://doi.org/10.3390/ijerph192416837.
[75] Lourenço A, Pereira H. Compositional variability of lignin in biomass. Lignin-Trends Appl 2018:65–98.
[76] Luo Y, Li Z, Li X, Liu X, Fan J, Clark JH, et al. The production of furfural directly from hemicellulose in lignocellulosic biomass: a review. Catal Today 2019;319:14–24. https://doi.org/10.1016/j.cattod.2018.06.042.
[77] Machado G, Leon S, Santos F, Lourega R, Dullius J, Mollmann ME, et al. Literature review on furfural production from lignocellulosic biomass. Nat Resour 2016;07:115–29. https://doi.org/10.4236/nr.2016.73012.
[78] Li X, Jia P, Wang T. Furfural: a promising platform compound for sustainable production of C4 and C5 chemicals. ACS Catal 2016;6:7621–40. https://doi.org/10.1021/acscatal.6b01838.
[79] Lange JP, Van Der Heide E, Van Buijtenen J, Price R. Furfural-a promising platform for lignocellulosic biofuels. ChemSusChem 2012;5:150–66. https://doi.org/10.1002/cssc.201100648.